

# Analysis of the Effect of Trailer Tire Size on the Articulated Vehicle's Stability

Glenn Xavier Vaz, Zeinab El-Sayegh

Department of Automotive and Mechatronics Engineering, Ontario Tech University, Oshawa, Canada

Email: [Zeinab.el-sayegh@ontariotechu.ca](mailto:Zeinab.el-sayegh@ontariotechu.ca)

**How to cite this paper:** Vaz, G.X. and El-Sayegh, Z. (2023) Analysis of the Effect of Trailer Tire Size on the Articulated Vehicle's Stability. *Journal of Applied Mathematics and Physics*, **11**, 2343-2360. <https://doi.org/10.4236/jamp.2023.118150>

**Received:** July 19, 2023

**Accepted:** August 18, 2023

**Published:** August 21, 2023

Copyright © 2023 by author(s) and Scientific Research Publishing Inc.

This work is licensed under the Creative Commons Attribution International License (CC BY 4.0).

<http://creativecommons.org/licenses/by/4.0/>



Open Access

## Abstract

This research paper aims to identify the effect of tire size on the handling characteristics of a trailer attached to a vehicle. In various stability tests, different models with different tires from the market were tested. A successful outcome of this research would generate an efficient tire selection process and improve the handling of a trailer attached to a vehicle while maximizing fuel efficiency. In this study, different accurate tire models using the magic formula were developed in vehicle dynamics modelling and simulation software. These models were then simulated on on-road conditions to predict vehicle and trailer behaviour under different conditions within the software. Two distinct tests were conducted, the J-Turn test and the Double Lane change test. The results of these tests were used to evaluate the handling characteristics and decide on a better tire size for the trailer attached to the vehicle.

## Keywords

Trailer-Vehicle, Slip Angle, Lateral Forces, Lateral Acceleration J-Turn, Double Lane Change

## 1. Introduction

Tires form an integral unit in road vehicle handling. As the only part of the handling system in contact with the ground, it determines whether the vehicle handles well or badly. In this study, we are going to examine the Compact Recreational Vehicle (RVs) trailer. These are wheeled living spaces without onboard propulsion and are towed by another vehicle. Considering that the vehicle in front provides propulsion and the unit of contact between the vehicle and the trailer is one point, the chosen tires are especially important in these vehicles, because the load of the whole vehicle lies on two tires and the point the trailer is

attached to the vehicle. With the use of compact RVs growing exponentially in recent times, the research on its dynamics, although huge, is not complete. Several characteristics of the articulated vehicle have been studied and analyzed to determine their influence on vehicle stability; however, the tire size is rarely analyzed.

Recently in 2022, Hao *et al.* [1] investigated the effect of reinforcement and permeability of the gravel-tire chips mixture for marine landfill application. The study proposes an economical construction method using a gravel-tire chips mixture as the horizontal reinforcement and drainage medium beneath the waste. The study concluded that the gravel-tire chips mixture performs better than the sand, a traditional reinforcement material.

Multiple studies have been conducted on articulated vehicles. In 2021, Lei *et al.* [2] established a linearized stability model to analyze the stability of articulated vehicles. With the help of several vehicle state parameters, the objective and subjective causes of snake oscillation as well as relevant indicators of snake instability were analyzed. Combining the eigenvalue method with multiple state parameters allowed them to do so. They discovered that the center of mass position had a more substantial influence on the stability. One limitation of the research was the linearization of the equation of state, where higher values of swing values would make it no longer appropriate.

In 2021, Bako *et al.* [3] presented a literature review on the stability analysis of a semi-trailer articulated vehicle. A bicycle model was used as the basis of their research. The effects of different factors like the height of the center of gravity (CG) from the ground, the distance of the CG from the hitch, etc. on different aspects of the vehicle was presented. A study of the dynamic stability, yaw stability, lateral stability, rollover stability, CG position, and the articulated vehicle's speed stability was presented. They have tabulated all their findings and literature review in the paper.

The relationship between the road and the articulated vehicle was also intensively researched. In 2019, AS Mendes *et al.* [4] presented the influence of the road tire coefficient on the yaw stability of the vehicle. They used a nonlinear 4 DOF model to present the estimation of the convergence, non-rollover and non-jackknifing regions using the phase trajectory method and a large number of simulations. The research concluded that for low coefficient values, no rollovers will occur and for high coefficient values, no jack-knifing will occur. A detailed assessment of the transition region is presented in this paper. In 2012, Tabatabaei *et al.* [5] studied the effects of the cornering stiffness on the articulated vehicle's stability using analysis and simulations. A linear model was used to analyze the vehicle's dynamic stability and a non-linear model was used to evaluate the predicted results derived from stability analysis. The effect of the change of cornering stiffness on different axles was presented in this paper. In 2010, Iida *et al.* [6] conducted a systematic and experimental approach to the measurement and analysis of the side slip angle of an articulated vehicle. The vehicle used for the experiment was a wheel loader (Caterpillar 910 G; 63 kW) with

a pivot joint and two axles. The experiment was a circular path test with an articulated angle of 34 deg and a constant speed range of 1.0 - 2.5 m/s. The experimental results of the side slip angle, speed and yaw rate were then compared to the simulated results and the mathematical results.

In 2005, He *et al.* [7] conducted a stability analysis of an articulated vehicle. They used a 2 DOF bicycle model, a 3 DOF model and a hybrid model, including a hydraulic power steering sub-model, dynamic tire sub-model and a mechanical vehicle sub-model to conduct the tests. Numerical simulations were used with the 2 DOF model as a reference, to investigate the effects of design variables on the stability of the vehicles. The research mainly highlighted that when the vehicles followed Ackerman steering mechanisms, three modes of risks were identified. These are 1) Snaking (oscillation of trailer yaw); 2) Jack-Knifing (Yaw motion of vehicle) and 3) Trailer Swing (yaw motion of trailer). These motions are illustrated in **Figure 1**.

If these situations arise, the safety of the driver and vehicle is compromised. It is also a risk hazard to the other vehicles in proximity. In some extreme cases, the vehicle and trailer can tip over to the side, causing a major accident. Choosing the right tire leads to better handling, improved fuel efficiency and higher safety factors for the driver, the passengers and the vehicles around it.

To determine the stability of the vehicle, a 2 DOF “bicycle” model is considered as illustrated in **Figure 2**.

To ensure the vehicle takes a turn safely, the understeer coefficient  $K$ , needs to be close to zero. From Equation (1) [8], we can determine that a low Cornering Stiffness coefficient is important to ensure a good understeer coefficient.

$$K = \left[ \left( \frac{1}{C_{\gamma 1}} + \frac{1}{C_{\gamma 2}} \right) (b + e) m_2 + (m_1 + m_2) \left( \frac{a}{C_{\gamma 2}} - \frac{b + L_2}{C_{\gamma 1}} \right) \right] / (L_1 + L_2)^2 \quad (1)$$

where “ $C_{\gamma 1,2}$ ” are the Cornering stiffness coefficient of the front (1) and back (2), “ $m_{1,2}$ ” is the mass of the driving vehicle (1) and trailer (2), “ $L_{1,2}$ ” is the length of the driving vehicle (1) and trailer (2), “ $a$ ” is the distance from the front axle to the CG of the vehicle, “ $b$ ” is the distance from the CG to the rear axle and “ $e$ ” is the distance from the front axle of the trailer to its CG.

As illustrated in **Figure 3**, the slip angle has a “Peak Lateral Force Slip angle”. Any angle beyond this is going to cause the vehicle to lose adhesion to the road and make the trailer-vehicle combination lose control. Therefore, it is important to bring the angle as close to the Peak Lateral Force Slip angle as possible. According to Equation (2) [9], the Cornering Stiffness ( $C_\alpha$ ) for slip angle ( $\alpha$ ), is directly proportional to the Lateral Force ( $F_{y\alpha}$ ).

$$F_{y\alpha} = C_\alpha \alpha \quad (2)$$

The cornering stiffness is defined as the rate of change of the cornering force at zero slip angle:

$$C_\alpha = \left. \frac{\partial F_{y\alpha}}{\partial \alpha} \right|_{\alpha=0} \quad (3)$$

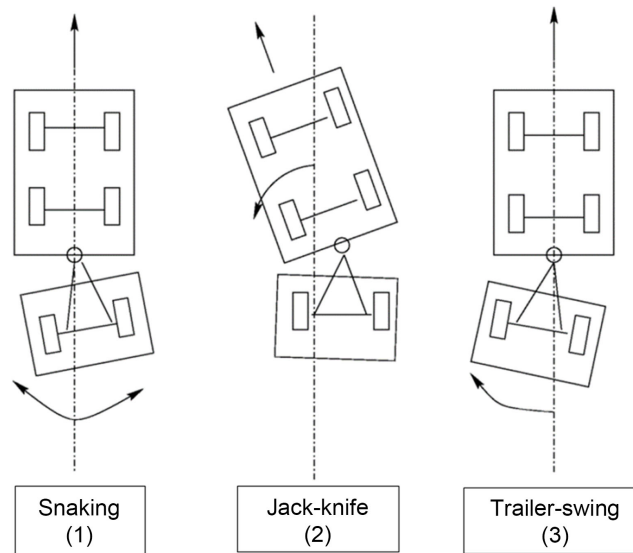


**Figure 1.** Unstable motion modes of traditional articulated vehicles [7].

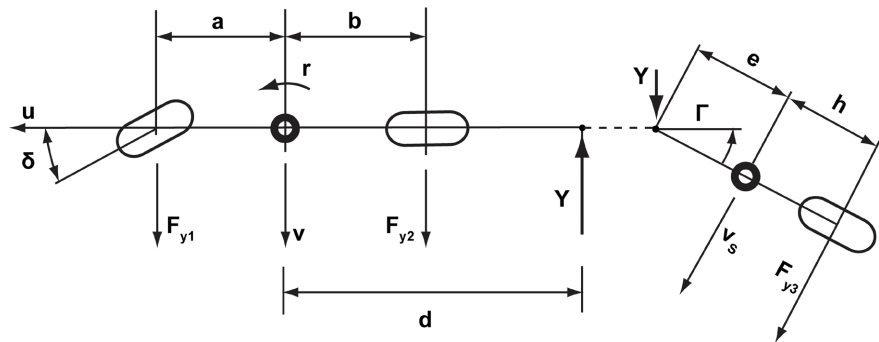


**Figure 2.** 2-Degree of Freedom (DOF) "Bicycle model" [8].

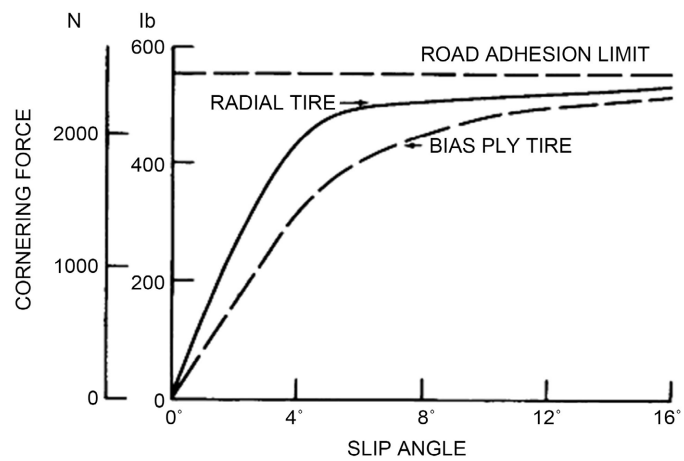


**Figure 3.** Cornering Force vs Slip Angle for Radial and Bias ply tire [8].

Therefore, to attain a very low cornering stiffness coefficient, the Lateral forces need to be as low as possible. In the following sections, the vehicle models for the

different tire sizes are run through a TruckSim simulation and modelling software simulation. These models will be compared and studied on the basis of the two pre-mentioned characteristics.

This research paper aims to provide insights into the effect of tire size on the handling characteristics of a trailer attached to a vehicle through an extensive sensitivity analysis. Several stability tests and different models with different tires from the market are examined and investigated. This research also generates an efficient tire selection process and improves the handling of a trailer attached to a vehicle while maximizing fuel efficiency.

## 2. Methodology

Modeling and simulation software TruckSim v2022.0 [10] was used for the following research. It is chosen for its standalone nature, large library, and built-in controllers for performing a variety of tests. The computer system that ran this software was powered by an AMD Ryzen 7 6800H processor with 16.0 GB RAM and a 64-bit operating system. Data from the tests conducted were read, analyzed, and plotted into graphs using Microsoft Excel 2021.

To begin with, relevant research was conducted to select the driving vehicle model, the trailer model, and the tires. This included researching different prospects from various journal articles and articles. A generic European van was chosen as the driving vehicle, and a one-axle hitch trailer was chosen as the trailer. The following sections explore these models in more detail. In this study, touring tires were selected as the tires. A later section of the paper discusses the different tires.

TruckSim's easy-to-use interface made the methodology relatively simple. Using the appropriate specifications, driving vehicles and trailers were first designed. After that, three different models of the articulated vehicle were created, each with a different type of tire. As soon as the designs were finalized, the models with different tires were subjected to two lateral stability tests. There were two tests: the J-Turn test and the double lane change test. In the following sections, we explore the details and specifications of these tests. After the tests were conducted, to demonstrate the differences between the three models, the data from these tests were exported to Microsoft Excel for analysis and presentation in a graphical format. The results of this study are presented below. The flowchart in **Figure 4** illustrates how the methodology was applied.

## 3. Model Creation

In the following section, three distinct models are created. Each model has a driving vehicle (which provides the thrust to the system) and a trailer attached to its rear. The difference between the three models is the sizes of the tires that support the trailer. The sizes chosen are discussed in the section below. TruckSim modelling and Simulation software [10] were used to obtain the various models.

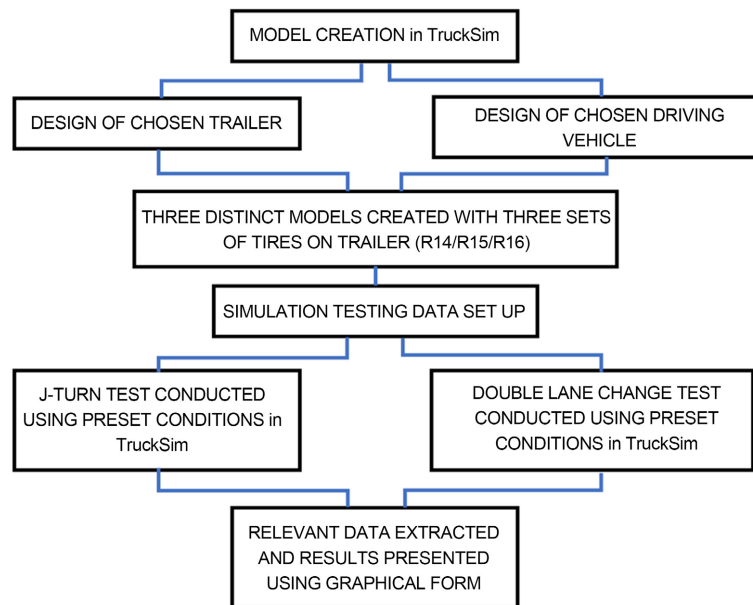


**Figure 4.** Methodology flowchart for TruckSim Model.

### 3.1. Driving Vehicle Model Specifications

The vehicle model chosen for the study was a generic large European van which is depicted in **Figure 5**. The vehicle is a two-wheel drive vehicle with it experiencing engine torque. The specifications are summarized in **Table 1**. The vehicle is powered by an internal combustion diesel engine providing 150 kw of power and 3000 rpm. The internal transmission powertrain was a 5-speed control with 3100 rpm and had a gear ratio of 3.91:1. The two axles of the vehicles have the same tires on both sides. The steering axle (front) has 390 mm steer tires. The tire has a width of 215 mm with a load rating of 2000 kg. The driven axle (rear) has dual 390 mm drive tires on either side. The specifications remain the same as the front, with a spacing of 310 mm.

### 3.2. Trailer Model Specifications

The trailer chosen for the study was a 1 Axle Rental Trailer. Its specifications are listed in **Table 2**. The model was available in the TruckSim software library. The trailer had a ground clearance of 565 mm. The vehicle tires did not have any toe in/out or any camber on them. The trailer did not have any brakes of its own and relied on the braking force provided by the vehicle. The lone axle of the trailer had a wheelbase of 1.95 m and was 2.86 m behind the pivot point. The payload applied to the whole trailer was a cuboid of 200 kg and had its center of gravity 2.5 m from the pivot.

### 3.3. Tires Specification

For the study, different tire sizes were researched. Touring tires were chosen for their common availability and their versatile use. These tires provide a comfortable ride and all-season-long traction along with responsive handling [11]. Three

touring tires of the same company were chosen: 175/65 R14; 215/70 R15 and 255/70 R16. The nomenclature for a tire is depicted in **Figure 6**. For the remainder of the paper, these tires will be referred to as the R14, R15 and R16 respectively. Each tire's characteristics are highlighted in **Table 3**. The tire models were attained from the TruckSim software library. Three models were created and subjected to simulation testing.

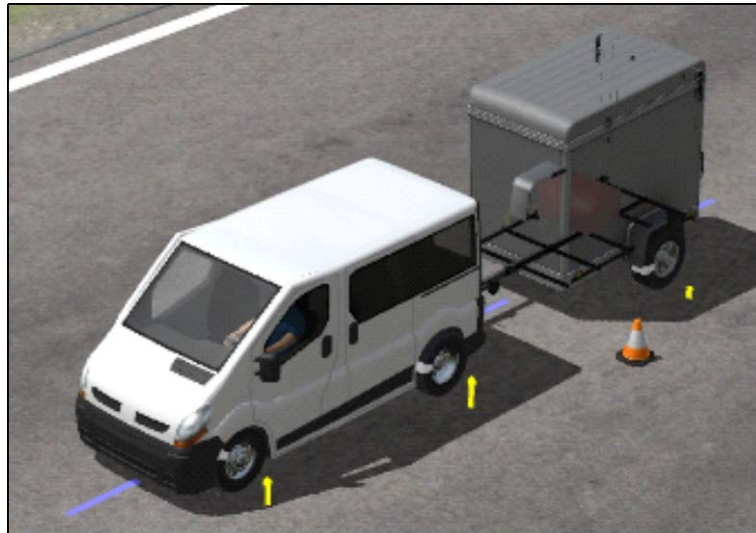


**Figure 5.** Combined view of the complete model in simulation.

**Table 1.** Driving vehicle specifications.

Characteristic	Value
Length	4900 mm
Width	2262 mm
Height	1960 mm
Center of gravity position	170 mm from the ground; 1350 mm from the front
Sprung mass	2100 kg
Roll Inertia	1029 kg/m <sup>2</sup>
Pitch Inertia	4116 kg/m <sup>2</sup>
Yaw Inertia	41,166 kg/m <sup>2</sup>
Radius of Gyration (Rx)	0.7 m
Radius of Gyration (Ry)	1.4 m
Radius of Gyration (Rz)	1.4 m
Length of axles	1625 mm (axle 1); 1550 mm (axle 2)
Distance between axles	3100 mm
Length	4900 mm
Width	2262 mm

**Table 2.** Trailer specifications.

Characteristic	Value
Height	2250 mm
Width	2100
Distance of Center of Gravity (from the ground)	971 mm
Distance of CG from hitch	2000 mm
Sprung mass	465 kg
Roll Inertia	708 kg/m <sup>2</sup>
Pitch Inertia	1810 kg/m <sup>2</sup>
Yaw Inertia	1764 kg/m <sup>2</sup>
Hitch type	Single-point Ball Hitch joint
Hitch distance	4100 mm (from the back)
Hitch height	500 mm (from the ground)
Height	2250 mm
Width	2100
Distance of Center of Gravity (from the ground)	971 mm
Distance of CG from hitch	2000 mm

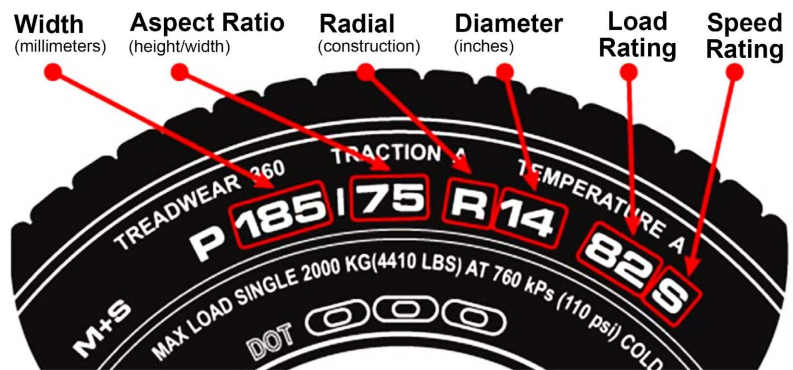


**Figure 6.** Tire nomenclature guide [11].

**Table 3.** Specifications of tires used.

Characteristic	R14	R15	R16
Radius	14 inches	15 inches	16 inches
Reference Vertical load	2200 N	8000 N	11,500 N
Effective Roll Radius	284 mm	329 mm	379 mm
Unloaded radius	292 mm	341 mm	394 mm
Spring Rate	230 N/mm	330 N/mm	470 N/mm
Mass	15 kg	22 kg	28 kg
Spin Moment of inertia	0.8 kg-m <sup>2</sup>	1.2 kg-m <sup>2</sup>	1.7 kg-m <sup>2</sup>
Width	175 mm	215 mm	255 mm
Contact patch dimensions	70 mm	90 mm	80 mm



Classically the tires are modelled using the “Magic Formula” for smooth road handling. The Magic Formula is not a predictive tire model but is used to empirically represent and interpolate previously measured tire force and moment curves. The Magic Formula for the longitudinal force is described as [12]:

$$Y(X) = D \cdot \sin \left[ C \arctan \left( B \cdot x - E \left( B \cdot x - \arctan Bx \right) \right) \right] \quad (4)$$

where:

$$Y(X) = y(x) + S_v \quad (5)$$

$$x = X + S_h \quad (6)$$

It should be noted that  $S_v$  and  $S_h$  are the vertical and horizontal shifts, respectively. In this case,  $Y$  is either the side force  $F_y$ , the aligning moment  $M_z$  or the longitudinal force  $F_x$  and  $X$  is either the slip angle  $\alpha$  or the longitudinal slip, for which Pacejka uses  $\kappa$ .

#### 4. Simulation Set-Up

The simulation was carried out using TruckSim simulation and modelling software. TruckSim delivers the most accurate, detailed, and efficient methods for simulating the performance of multi-axle commercial and military vehicles. It is widely used to analyze vehicle dynamics, develop active controllers, calculate a truck’s performance characteristics, and engineer next-generation active safety systems.

In order to determine the handling characteristics, the models were subjected to the two following tests.

##### 4.1. J-Turn Test Method

This method is used to test a vehicle’s dynamic anti-roll properties [13]. It demonstrates the roll stability of the vehicle, and its ability to avoid obstacles in an emergency. This is deemed as one of the worst driving conditions.

For the test, the vehicle was subjected to an initial speed of 50 km/h, with a steering input of 294 degrees applied in the right direction. The vehicle experiences a change of 720 deg/s and holds the steering angle for 0.26 sec. This is followed by a second counter-steer angle of 588 degrees to bring the steering angle to -294 degrees. The steering angle changes at 720 deg/s and is maintained for 2.5 sec. The last steer angle is applied, bringing the steering angle to zero. The steer wheel input angle for the J-Turn test is shown in **Figure 7**. The top view of the simulated J-Turn test conducted is depicted in **Figure 8**.

For this study, tests were run for each of the tire models and the following values were attained from the simulation: Force acting on the left tire of the trailer ( $F_{y_L}$ ); Force acting on the right tire ( $F_{y_R}$ ), the lateral acceleration of the vehicle ( $A_v$ ) and the trailer ( $A_t$ ); and the sideslip angle of the vehicle ( $\beta_v$ ) and the trailer ( $\beta_t$ ) attached behind.

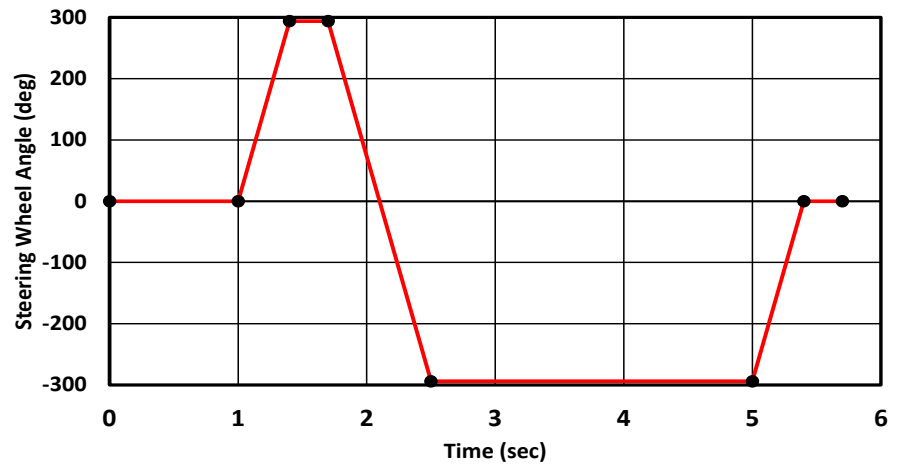


**Figure 7.** Variation of steering wheel angle (degree) with time (seconds).

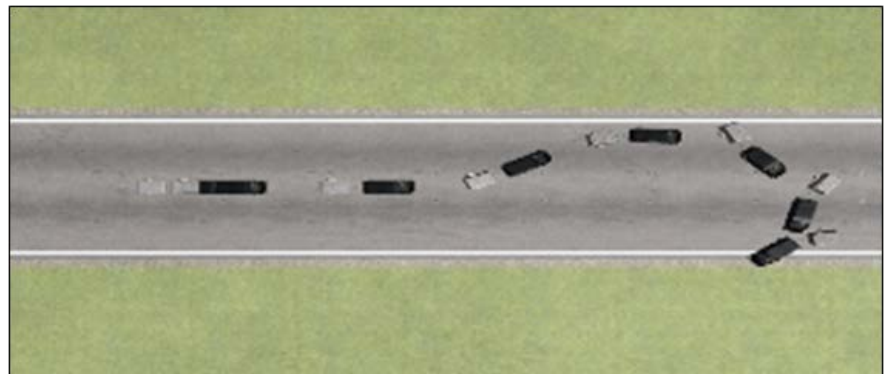


**Figure 8.** Top View of the J-Turn test conducted in TruckSim.

## 4.2. Double Lane Change Test

The Double Lane Change maneuver is one of the best tests for performance evaluation [14]. It tests the vehicle's road stability and subsequently determines the road safety of the driver, the driving vehicle, the surrounding vehicles, and the passengers in them.

For the test, the vehicle is accelerated to a target speed of 80 kmph. Once the target speed is met, the maneuver occurs. The vehicle-trailer combination is subjected to a lateral offset of 3.5 m from the station in 20 m. This is the first lane change maneuver. The lateral offset is maintained for 25 m of the vehicle's longitudinal distance. Then a steering angle is applied to bring the vehicle-trailer combination back to its station, which is the second lane change maneuver. The graphical representation of the combination's position for the double lane change test is depicted in **Figure 9**.

For this study, tests were run for each of the tire models and the following values were attained from the simulation: Force acting on the left tire of the trailer ( $F_{Y_{L2}}$ ); Force acting on the right tire ( $F_{Y_{R2}}$ ), the lateral acceleration of the vehicle ( $A_{L2}$ ) and the trailer ( $A_{R2}$ ); and the sideslip angle of the vehicle.

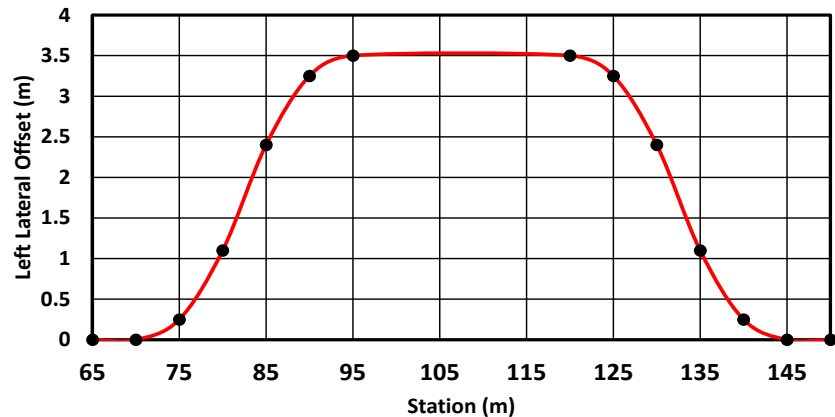


**Figure 9.** Variation of steering wheel angle (degree) with time (seconds).

## 5. Results and Discussions

The simulation results were exported to an Excel file. The data was sorted, and the required information was extracted. This was then depicted using line graphs in Microsoft Excel.

### 5.1. J-Turn Test Results

**Figure 10** shows the variation of the lateral forces acting on the right tire as a function of time. The graph has two peak values, with the R16 tire having the maximum values between 1 - 3 sec (Region A) with 5188 N and in between 6.5 - 8 sec (Region B) with 3778 N at 2.3 sec and 6.85 sec respectively. The R15 tire has a maximum force of 4908 N in Region A and 3429 N in Region B. The R14 tire experiences a maximum force of 4660 in Region A and 2940 N in Region B.

In **Figure 11**, the lateral force acting on the left tire is depicted in relation to time. The graph has peak values on either side for the R16 tire (5981 N & 1926 N). At A, the R16 tire experiences a large spike in the force. The R15 tire has a maximum force of 5635 N on one side and a maximum of 2050 N on the other side. The R14 tire experiences a maximum force of 5467 in Region A and 1444 N in Region B. However, in Region B, the maximum force for the R15 tire is slightly more than the R16 tire (by 124 N).

As a function of time, **Figure 12** illustrates the variation of the lateral acceleration acting on the driving vehicle. The three tires display similar characteristics for up to 5 seconds. When the car stops moving, lateral acceleration is induced in the vehicle due to the trailer's moment of inertia at the hinge. This causes a spike in the lateral acceleration of the vehicle. The R14 tire causes the most lateral acceleration with 0.634, followed by the R15 tire with 0.55 and finally the tire with the least acceleration R16 at 0.38.

**Figure 13** illustrates how the lateral acceleration acting on the trailer varies over time. The acceleration of the trailer remains similar for all three tires for the first turn (up to 3.25 sec). At A, the R16 tire experiences the most lateral acceleration of 0.99, compared to R15 (0.90) and R14 (0.87). The graph remains simi-

lar for the remainder of the test, with similar peak values on both sides. However, after 5.5 sec, there is a delay between the peaks. For example, in B, the peak for the R16 tire (0.44) occurs earlier at 6.675 sec. It is followed by the R15 tire (0.45) at 6.8 sec and then finally the R14 tire (0.44) at 7.1 sec.

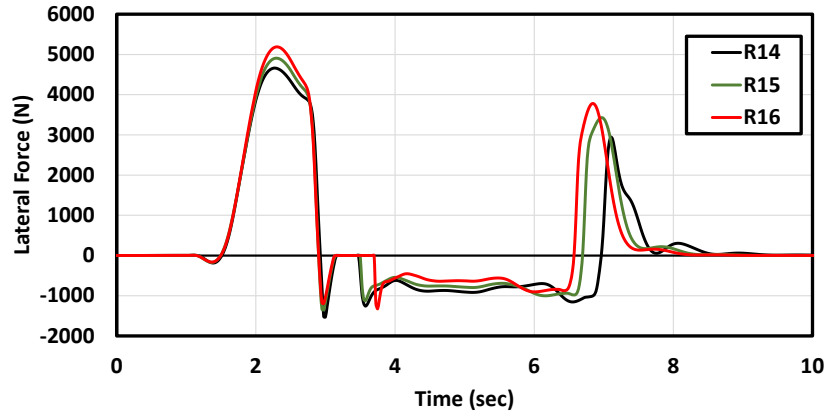


Figure 10. Variation of lateral force acting on the right trailer tire vs time (J-Turn test).

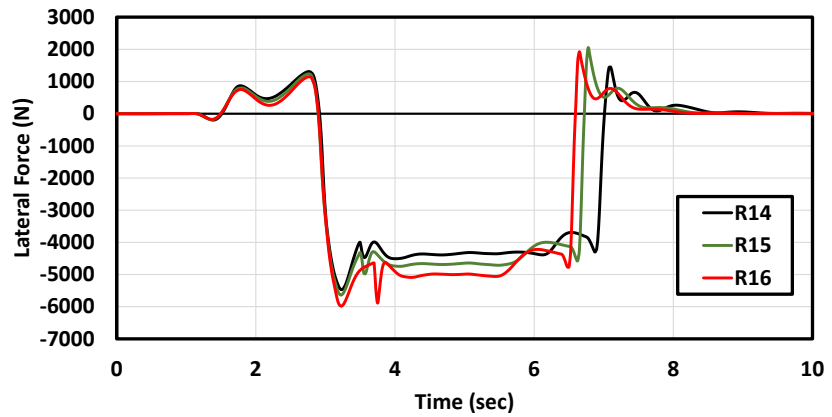


Figure 11. Variation of lateral force acting on the left trailer tire vs time (J-Turn test).

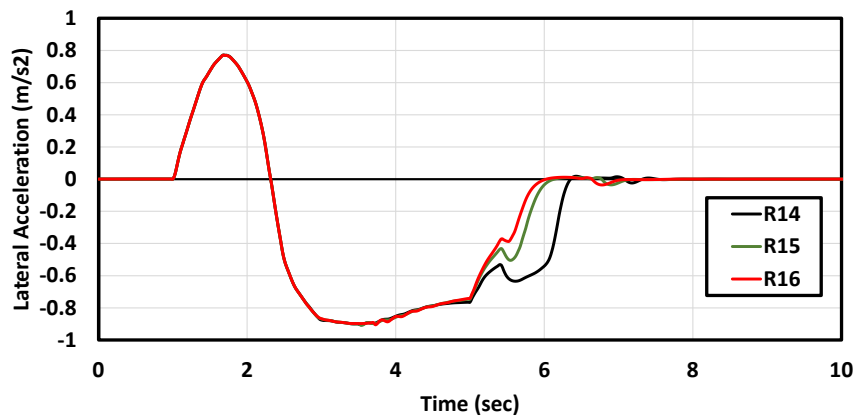
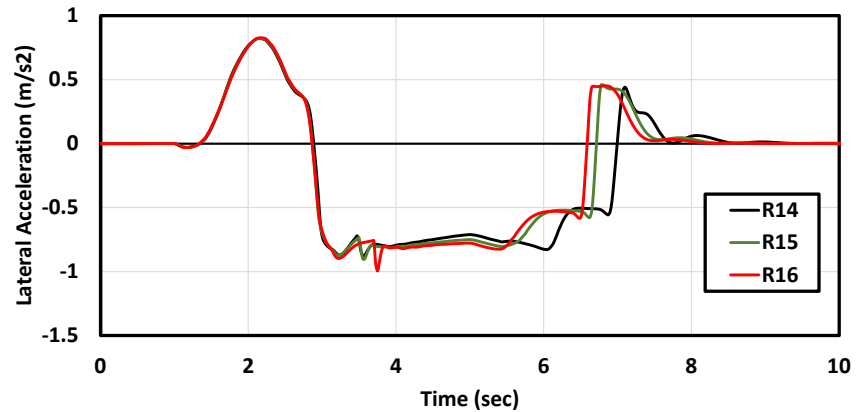


Figure 12. Variation of lateral acceleration on driving vehicle vs time (J-Turn test).



**Figure 13.** Variation of lateral acceleration on trailer vs time (J-Turn test).

The side slip angle of the driving vehicle is shown in **Figure 14** as a function of time. This graph depicts the effect of the trailer on the slip angle of the car. The graphs for all three tires remain similar up to 4 sec. After which, the side slip angle for the R14 tire peaks at 15.64 degrees. The R15 tire peaks at 7.5 deg followed by the least peak from the R16 tire with 4.9 deg. The peak for the R14 tire is more than three times the peak of the R16 tire.

**Figure 15** shows the variation of the side slip angle of the trailer as a function of time. The graphs of all three tires remain similar for up to 3 seconds. After which, the R14 tire obtains the highest peak at 61.95 deg. It takes the R14 tire longer to return to zero (8 sec). The R15 tire peaks at 57.51 deg followed by the least peak of the test, the R16 tire (53.85 deg).

**Figure 16** presents the deviation of the articulated vehicle from the intended path for the three types of tires on a coordinate system. For this test, the paths followed by the three models were compared with the path of a base model with no trailer attached. The path of the vehicle with no trailer was taken as the intended path. From the J-Turn test paths for the three tires, the R14 tire experiences the highest deviation from the intended path with 51.6 deg. This is followed by the R15 tire at 21.5 deg. The R16 tires offer the least deviation from the path at 14.52 deg.

## 5.2. Double Lane Change Test Results

For the Double Lane Change test, **Figure 17** shows the variations in the lateral force acting on the right tire over time. The graph for all three tires shows continuous variations. This is because the trailer never becomes stable before the next maneuver is executed. This is called “snaking”. For the right tire of the trailer, the highest peak is observed for the R16 tire (5959.69 N). It also has the highest variation of the forces (4246.5 N). The R15 tire comes in second with a maximum force of 5549.57 N and a range of 3624.64 N. The R14 tire has the lowest peak of 5193.1 N and the lowest range of 3044.118 N.

In **Figure 18**, the lateral forces acting on the left tire are plotted against time for the Double Lane Change test. The graph for the left tire, like the right one,

shows continuous variations because the trailer never becomes stable before the next maneuver happens. Like the right tire, the R16 tire experiences the highest peak force (5963 N) and largest range (4604.9 N). The R15 tire experiences a peak force of 5650.35 N and a range of 4063.12 N. The R14 tire experiences the lowest peak with 5618 N and a range of 3706.1 N.

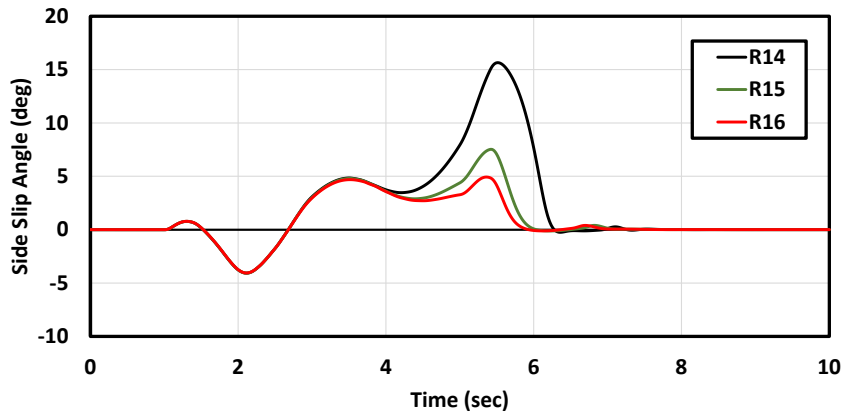


Figure 14. Variation of Side slip angle of driving vehicle vs time (J-Turn test).

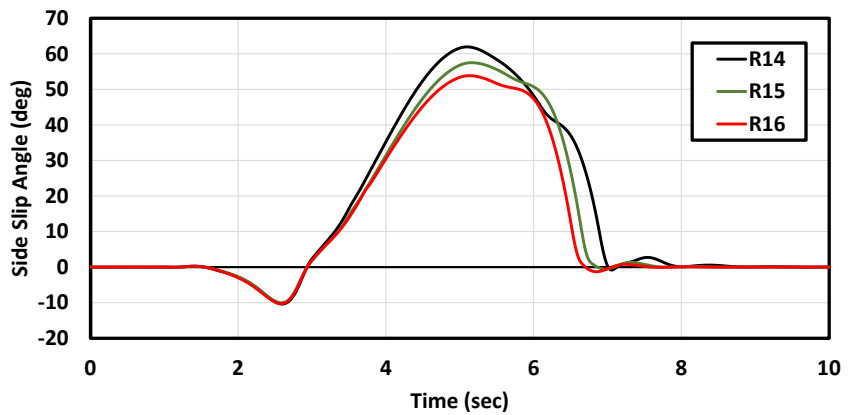


Figure 15. Variation of Side slip angle of trailer vs time (J-Turn test).

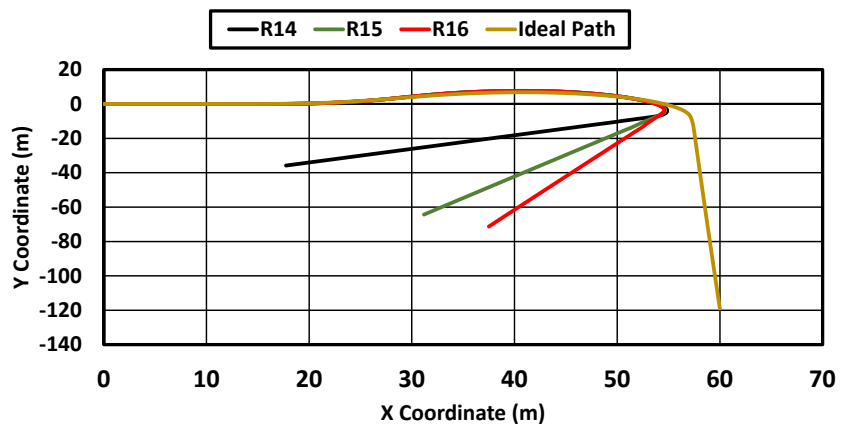
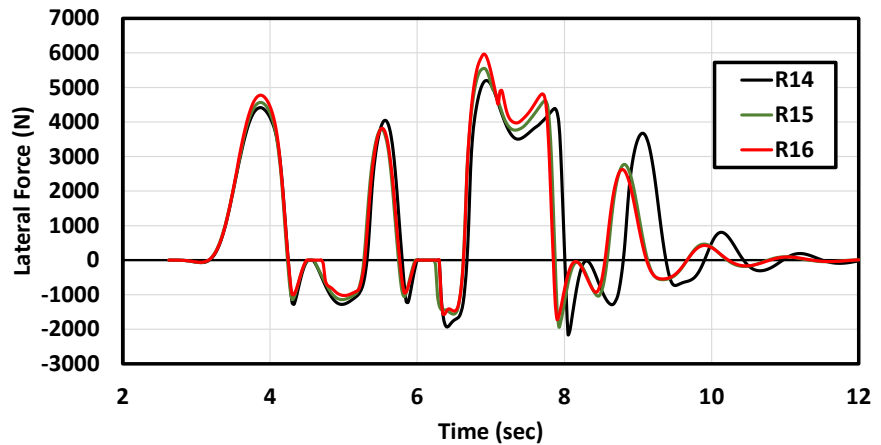
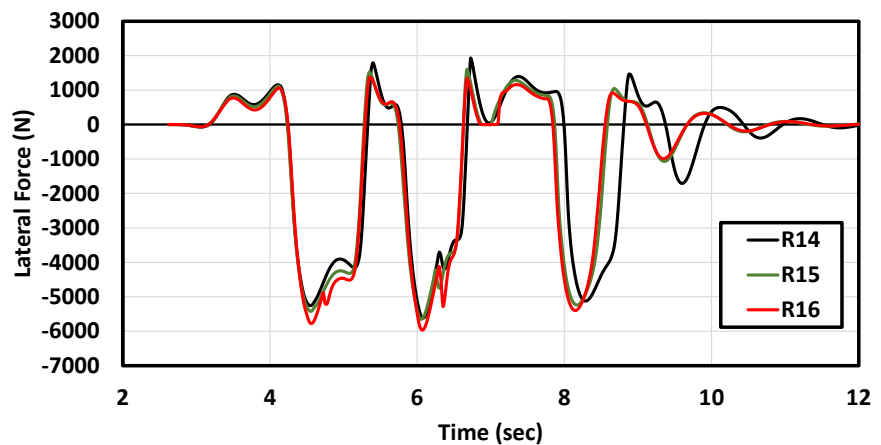


Figure 16. The path followed by articulated vehicle (J-Turn test).



**Figure 17.** Lateral Force acting on right tire vs time (DLC test).



**Figure 18.** Lateral Force acting on left tire vs time (DLC test).

Based on the Double Lane Change test, **Figure 19** illustrates the variation of the lateral acceleration acting on the trailer over time. In all three cases, the variation of the lateral acceleration of the vehicle remains similar. Even in the case of the trailer, the peak values on both sides remain similar (0.793/0.796 for R14, 0.796/0.80 for R15 and 0.799/0.81 for R16). However, towards the end (after 8.5 sec), the variation of the R15 tire and R16 follow a similar trend. But the variation of the R14 tire is more, indicating that the trailer experiences more “snaking” for the R14 tire.

**Figure 20** shows the variation of the side slip angle of the trailer as a function of time, for the Double Lane Change test. The variation in the slip angle of the trailer follows a similar trend for the R16 and R15 tires. The R16 trailer experiences a peak value of 21.52 degrees of slip with a range of 33.63 degrees while the R15 tire experiences a peak of 22.24 degrees in slip with a range of 33.89 degrees. The R14 tire experiences the highest slip with the peak value being 26.03 deg and variation being 38.885 deg.

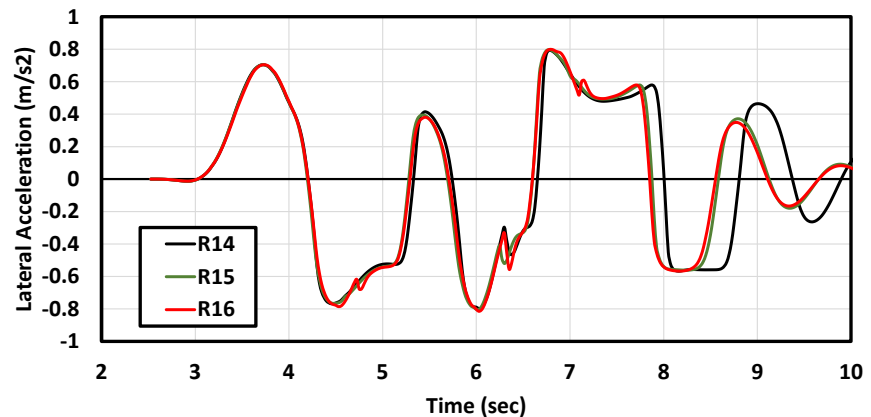


**Figure 19.** Lateral Acceleration on the trailer vs time (DLC test).

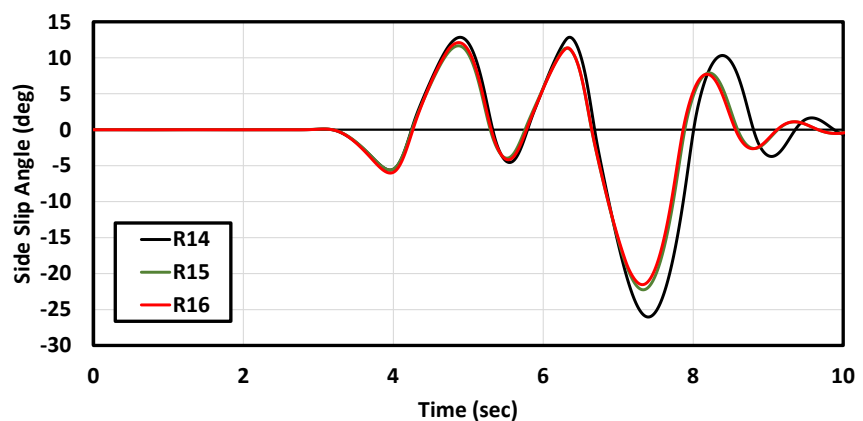


**Figure 20.** Lateral Acceleration on the trailer vs time (DLC test).

## 6. Conclusions

For the research conducted, three models were first created in the modelling and simulation software, TruckSim. These models were then subjected to two different types of stability tests—the J-Turn test and Double Lane Change test. In both tests (J-Turn test and Double Lane Change test), the R16 tire had the highest peak of lateral forces acting on both tires. On the other hand, both tests indicated that the lateral forces were the least with the R14 tires. However, it did show tendencies of “snaking” towards the end of the Double Lane tests.

The Lateral Acceleration in both tests favored the R16 tires. It had the least spike of vehicle lateral acceleration in the J-Turn test. In the Double Lane test, all the tires displayed similar peaks and ranges; however, the R16 tire had less variation towards the end. This depicts that the chance of “snaking” is comparatively lesser than R15 and R14. The Lateral Acceleration of the R14 tires was 35% more than the R16 tires on the vehicle in the J-Turn test. It had similar peaks for the trailer in the same test. It had similar peaks in the Double Lane Change test to the other tires. However, it did have a lot of variation in the lateral acceleration, hinting towards the possibility of “snaking”.



The Side Slip Angles in all the tests indicated the R16 tire to be the best choice. It had the minimum peak and the lowest range in all tests. The R14 tire performed poorly in the J-Turn test, as it produced more than three times the slip produced by the R16 tire on the vehicle. It had the highest peaks and the largest ranges in all the tests. In the J-Turn test, the R16 tires produced the least deviation from the intended path, making it the optimum choice in the test.

In conclusion, the 255/70 R16 tire was the most suitable option among the three tires based on the tests performed in this study. The R16 tire model had the highest peaks of lateral force, the lowest slip angle peaks, and the least deviation from the J-Turn path, making it the better tire of the tires used in this study. In the future, further analysis can be done to determine the effect of tire size on fuel consumption and ride comfort.

### Conflicts of Interest

The authors declare no conflicts of interest regarding the publication of this paper.

### References

- [1] Hao, C., Hazarika, H. and Isobe, Y. (2022) Reinforcement Effect and Permeability Assessment of Gravel-Tire Chips Mixture (GTCM) for Use in Marine Landfill. *Open Journal of Civil Engineering*, **12**, 208-230. <https://doi.org/10.4236/ojce.2022.122013>
- [2] Lei, T., Wang, J. and Yao, Z. (2021) Modelling and Stability Analysis of Articulated Vehicles. *Applied Sciences*, **11**, 3663. <https://doi.org/10.3390/app11083663>
- [3] Sunday, B.A.K.O. (2021) Stability Analysis of a Semi-Trailer Articulated Vehicle: A Review. *International Journal of Automotive Science and Technology*, **5**, 131-140. <https://doi.org/10.30939/ijastech..855733>
- [4] Mendes, A.D.S., Fleury, A.D.T., Ackermann, M., Leonardi, F. and Bortolussi, R. (2019) Assessing the Influence of the Road-Tire Friction Coefficient on the Yaw and Roll Stability of Articulated Vehicles. *Proceedings of the Institution of Mechanical Engineers, Part D: Journal of Automobile Engineering*, **233**, 2987-2999. <https://doi.org/10.1177/0954407018812957>
- [5] Tabatabaei, S.H., Zahedi, A. and Khodayari, A. (2012) The Effects of the Cornering Stiffness Variation on Articulated Heavy Vehicle Stability. 2012 *IEEE International Conference on Vehicular Electronics and Safety (ICVES 2012)*, Istanbul, 24-27 July 2012, 78-83. <https://doi.org/10.1109/ICVES.2012.6294280>
- [6] Iida, M., Fukuta, M. and Tomiyama, H. (2010) Measurement and Analysis of Side-Slip Angle for an Articulated Vehicle. *Engineering in Agriculture, Environment and Food*, **3**, 1-6. [https://doi.org/10.1016/S1881-8366\(10\)80004-7](https://doi.org/10.1016/S1881-8366(10)80004-7)
- [7] He, Y., Khajepour, A., McPhee, J. and Wang, X. (2005) Dynamic Modelling and Stability Analysis of Articulated Frame Steer Vehicles. *International Journal of Heavy Vehicle Systems*, **12**, 28-59. <https://doi.org/10.1504/IJHVS.2005.005668>
- [8] El-Gindy, M. and El-Sayegh, Z. (2023) Road Vehicle Stability and Control. In *Road and Off-Road Vehicle Dynamics*, Springer International Publishing, Cham, 153-184. [https://doi.org/10.1007/978-3-031-36216-3\\_4](https://doi.org/10.1007/978-3-031-36216-3_4)
- [9] Wong, J.Y. (2022) *Theory of Ground Vehicles*. John Wiley & Sons, Hoboken.

- <https://doi.org/10.1002/9781119719984>
- [10] (2019) Mechanical Simulation, “TruckSim Overview”.  
<https://www.carsim.com/products/trucksim/>
- [11] (2023) Discount Tires, “Different Types of Tires”.  
<https://www.discounttire.com/learn/basic-tire-info>
- [12] El-Gindy, M. and El-Sayegh, Z. (2023) Road and Off-Road Vehicle Dynamics. Springer Nature, Berlin. <https://doi.org/10.1007/978-3-031-36216-3>
- [13] Xiong, F., Lan, F., Chen, J. and Zhou, Y. (2015) The Study for Anti-Rollover Performance Based on Fishhook and J Turn Simulation. *Proceedings of the 3rd International Conference on Material, Mechanical and Manufacturing Engineering*, Guangzhou, 27-28 June 2015, 2084-2093. <https://doi.org/10.2991/ic3me-15.2015.401>
- [14] Bîndac, I.M., Bradley, S., Roşca, P., Pupăză, C. and Giurgiu, T. (2022) Theoretical and Experimental Research on the Double Lane Change Maneuver. *MATEC Web of Conferences*, **373**, 00054. <https://doi.org/10.1051/mateconf/202237300054>